Proc. of the 9th Intl. Conf. of Asian Society for Precision Engg. and Nanotechnology (ASPEN 2022)
15–18 November 2022, Singapore. Edited by Nai Mui Ling Sharon and A. Senthil Kumar
doi://10.3850/978-981-18-6021-8_OR-06-0089

Eco-Friendly Direct Synthesis and Micro-Patterning of Copper on Flexible Transparent Substrates

Swami Siddharth#, Yu-Bin Chen, and Ming-Tsang Lee

Department of Power Mechanical Engineering, National Tsing Hua University, Hsinchu City, 30013 Taiwan, R.O.C.
Corresponding Author / Email: ssid.2460@gmail.com, TEL: +886-3-5733743

KEYWORDS: Copper-ion liquid precursor, Flexible conductors, Laser reductive sintering, Thermal treatment

Flexible electronics have gained significant attention in last few decades due to their applications in various devices. The liquid precursor-based laser-induced reductive technique provides a solution to a fast and low-cost fabrication of flexible conductors. In this study, we demonstrated the preparation of an eco-friendly and particle-free copper ionic solution. The solution was utilized as a precursor to fabricate copper microstructures on transparent and flexible polyethylene terephthalate (PET) using laser direct synthesis and patterning (LDSP) technique. Water was used as the solvent, while L-ascorbic acid, which is also known as Vitamin C, was used as the reducing agent. Both chemicals are environmentally benign and are not hazardous to human health. A suitable processing parameters window for fabricating Cu microlines on PET was evaluated based on the electrical resistance measurement of the copper micropatterns. We further investigated the improvement of the mechanical durability by laser reheating of copper microstructures as post-processing. Cyclic bending tests showed that the change in resistance of samples with post-processing after 1000 bending cycles was around 77% less than that of samples without post-processing. This improvement in flexibility was attributed to the enhancement in copper-PET interfacial adhesion, which was confirmed with pull-off test and SEM analysis. Apart from interfacial adhesion, post-processing also improved conductivity of the copper microstructures. Resistance of the copper microcline was reduced by up to 39% after post-processing which was attributed to grain growth during post-processing. Average grain size of copper microstructures was around 54% higher than that without post-processing. The resistivity of the fabricated copper micropattern was as low as 4.7 μΩ□cm with optimized laser parameters, which is only about three times of that for pure copper, and is among the best electrical property achieved by similar state-of-the-art micro-patterning technologies. In addition to deposition of conductive microstructures during LDSP, formation of microbubbles was found to be inevitable. In this regard, comprehensive investigation of bubble dynamics during LDSP would be useful in understanding underlying mechanism of bubble formation and its effect on properties of fabricated conductive microstructures. Therefore, in addition to investigation of conductivity and mechanical durability of fabricated Cu microstructures, preliminary results of bubble dynamics are also reported in this study. Results of this study pave the way for green and sustainable manufacturing of next generation flexible and wearable electronics with a rapid, economic, and low-energy-consumption process.

1. Introduction

Demand for smart devices, especially flexible electronics has increased in last few decades and is still increasing. Therefore, development of fabrication techniques for manufacturing flexible conductors has gained significant attention. These techniques are restricted to low temperature fabrication processes due to low glass transition temperature of the flexible substrates like polyethylene terephthalate (PET). Nanoparticle (NP) and nanowire (NW) based fabrication techniques are popular low temperature fabrication techniques which are simpler and having higher degree of design flexibility than conventional fabrication techniques like stereolithography [1]. However, these techniques are time consuming as it takes several hours to synthesize NPs [2] and to develop NWs [3]. Laser direct synthesis and patterning (LDSP) is alternative to NPs based fabrication technique which is utilized in the current study. LDSP is considered to be economic as it uses particle-free liquid based precursor which does not need to undergo synthesis unlike NPs based precursor. LDSP for fabricating silver microlines on PET film has already been studied [4]. However, advantages of silver based LDSP is outweighed by high cost of silver. In this regard, copper is considered to be the feasible alternative which is available at lower price than the silver. Moreover, most of the chemicals used in Cu-based precursor are hazardous to human health and environment. This study demonstrates the preparation of eco-friendly and particle-free Cu ionic precursor and fabrication of Cu microlines on transparent PET [5]. In addition, to improve the Cu–PET interfacial adhesion and the mechanical durability of the Cu microlines, laser reheating as post-processing was employed using the same laser source with a different set of parameters. In addition to fabrication of conductive microstructures and enhancing their mechanical durability, bubble dynamics during LDSP was also investigated. The preliminary results of bubble dynamics during LDSP is also reported in this study.

2. Experimental details

2.1 Preparation of eco-friendly and particle-free precursor

A transparent ascorbic acid solution as shown in Fig. 1(a) to be used as reducing agent was prepared by mixing 3 g of ascorbic acid in DI water at elevated temperature. Then, a blue coloured cupric acetate solution as shown in Fig. 1(b) was prepared by mixing 1 g cupric acetate in 5 mL of deionized water followed by addition of 0.4 mL formic acid to the mixture. Further, as prepared solutions were mixed in the ratio 1:1 by volume and filtered using syringe filter. An olive green colour particle-free copper ionic solution was obtained as shown in Fig. 1(c).

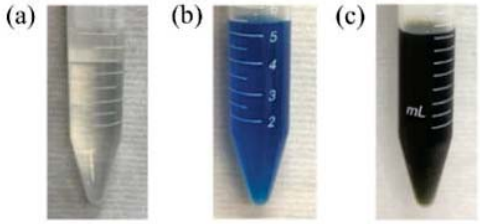

Fig. 1 (a) L-Ascorbic acid aqueous solution, (b) cupric acetate solution (in DI water with 6.5% in vol. of formic acid), and (c) particle-free copper ionic solution.

2.2 Experimental setup for LDSP

Figure 2 shows the schematic of experimental setup for LDS process and fabricated copper microstructure on PET, respectively. The precursor was evenly spread over PET kept on transparent glass. A continuous wave (CW) laser of 640 nm wavelength was focused at the solution-PET interface. Laser power used was 550 mW and the glass holder was moved to-and-fro along the straight line using motorized linear guideway with 1 mm/s. Enhanced localized temperature induces reduction reaction and Cu is deposited over the PET surface.

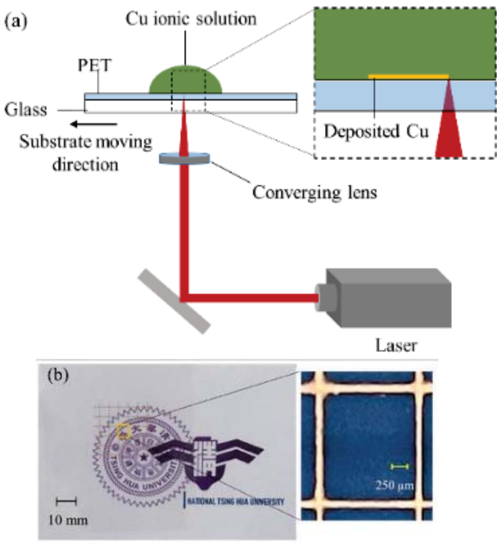

Fig. 2 (a) schematic of experimental setup for copper LDSP process, and (b) fabricated copper microstructures on PET.

3. Results and discussion

3.1 Fabrication of conductive microlines on PET

Figure 3 shows fabricated Cu microlines on PET with different number of LDSP scans and corresponding cross section profiles. Cross section profiles were measured using 3D profiler. The valley along the centerline of microlines shown in Fig. 3(b), is attributed to thermal deformation of PET, thermocapillary effect of thin metal film and its heterogenous interface with PET during laser heating [5]. Thickness of microline increases with number of scans till 20 LDSP which is due to self-limiting reaction due to increased reflection of laser beam from the fabricated microlines. Numerical simulation of heat and transport in the vicinity of the laser spot was conducted to estimate the reaction temperature by following the previously reported procedure [6] which was found to be 355 K.

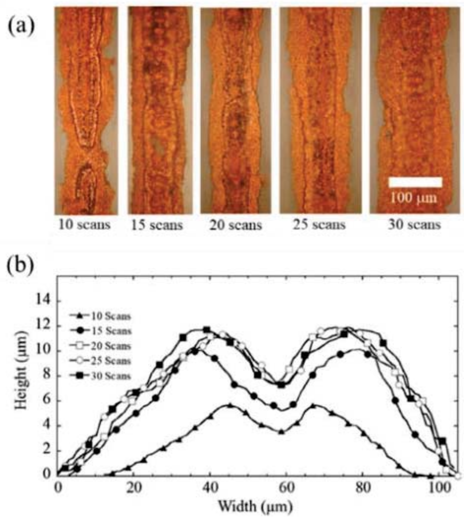

Fig. 3 (a) Copper microlines fabricated by LDSP with different number of scans and (b) corresponding average cross-section profiles.

3.2 Laser post-processing

3.2.1 Conductivity of fabricated Cu microline

Figure 4 shows the resistance of copper microlines fabricated with different number of LDSP scans with and without post-processing. Fabricated Cu microlines on PET were reheated with adjusted laser spot in order to cover the full width of the microline during scanning using 110 mW laser power and 10 scans. As shown in the figure, the resistance reduces with number of laser scans owing to increase in thickness of the microlines which becomes saturated after 20 scans. Furthermore, the post-processing reduces the resistance by ~71% for the sample with 10 LDSP scans. Post-processed samples showed very little reduction in resistance after 20 LDSP scans owing to deposition and annealing simultaneously at relatively higher LDSP scans. However, 10 postprocessing scans did reduce the electrical resistance of the 20 LDSP Cu microlines to an average of ~0.86 Ω. This was a value that could not be achieved without post-processing even with 30 LDSP scans. The resistivity of the fabricated copper microline achieved was as low as 4.7 μΩ□cm which is remarkably good compared with the resistivity of the bulk Copper (1.7 μΩ□cm).

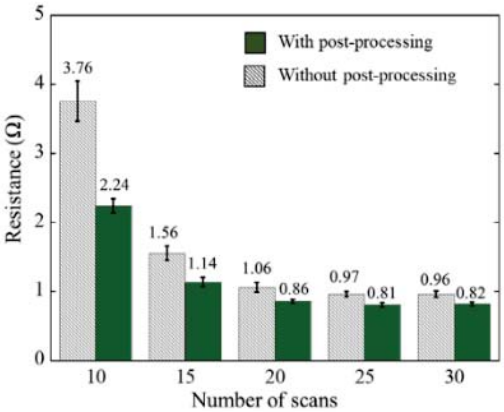

Fig. 4 Resistance of fabricated Cu microlines made with different numbers of LDSP scans with and without postprocessing

3.2.2 Mechanical durability

Figure 5 shows relative change in resistance ($\Delta R/R_0$) of copper microlines fabricated on PET with and without post-processing. ΔR is the difference of resistance of copper microline before and after the sample underwent bending cycle. R_0 is the resistance of the of the copper microline prior to bending test. Apart from conductivity, mechanical durability of fabricated conductive microstructure on flexible conductors is an important aspect as it undergoes mechanical deformation during its application. Mechanical durability of as prepared samples with and without post-processing was compared through cyclic bending test. Increase in resistance with increase in number of bending cycles is attributed to generation of microcracks which was confirmed through SEM analysis. Post-processing improved the mechanical durability of fabricated microlines which was evident from reduction of $\Delta R/R_0$ by up to 77%. Pull-off tests confirmed improvement in Cu-PET interfacial adhesion after post-processing which was the reason of enhanced mechanical durability. Normal pulling force during pull-off test for the sample with and without post-processing was found to be in the range of 720-880 N and 390-610 N, respectively.

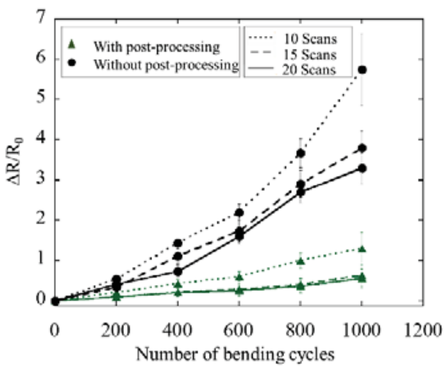

Fig. 5 Relative change in resistance ($\Delta R/R_0$) after a cyclic bending test of Cu microlines fabricated on PET with a different number of LDSP scans with and without postprocessing.

3.2.3 SEM analysis

Figure 6 shows SEM images of surface of copper microlines after as prepared samples underwent 1000 bending cycles and grain distribution for the cases with and without post-processing. As can be seen in the Fig. 6(a) and 6(b), surface of copper microlines without post-processing has more microcracks than that with post-processing. These microcracks were responsible for increase in resistance which was improved after post-processing. Furthermore, post-processing increases average grain size and decreases the grain boundaries, see Fig. 6(c) and 6(d). The average number of grains was measured as 0.61 and 0.94 μm^{-2} for Cu microline with and without post-processing, respectively, indicates ~54% increase in grain size. This increase in grain size is attributed to annealing of Cu microstructures during post-processing [7]. Reduced grain boundaries lowered electrical resistance in Cu microlines.

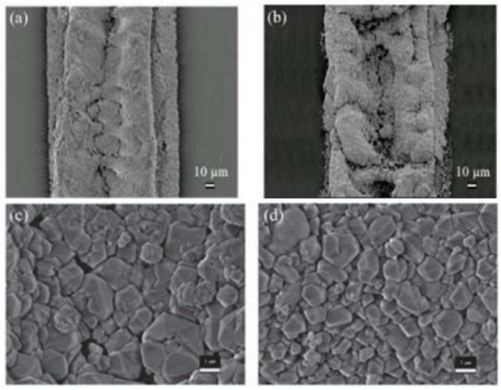

Fig. 6 SEM image of copper microstructures after 1000 bending cycles (a) with and (b) without postprocessing; and grain distribution for the Cu microline (c) with and (d) without post-processing.

Figure 7(a) and 7(b) show SEM images of Cu-PET interface of fabricated Cu microline on PET with and without post-processing, respectively. As can be seen in the figure, there are obvious voids (marked in red) available at Cu-PET interface for the case without post-processing while no noticeable voids are available for the case with post-processing. This result further confirms the improved Cu-PET interfacial adhesion after post-processing.

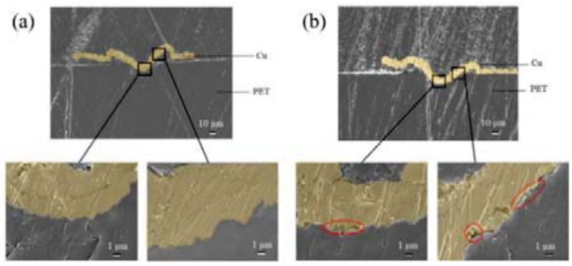

Fig. 7 Cross section and Cu–PET interface of fabricated Cu microlines on PET (a) with and (b) without post-processing.

Figure 8(a) and 8(b) show SEM and 3D profiler images of surface morphology if Cu microline on PET with and without post-processing, respectively. As can bee seen in 3D profiler images, surface of the Cu microline with post-processing is relatively smooth. Moreover, Cu microline with post-processing has fewer voids than that without post-processing. Surface smoothness indicates uniformity and solidity of the fabricated microline. Presence of voids i.e. pores also affect the electrical conductivity of the Cu microline which was improved after post-processing. Improved microstructure after post-processing is confirmed to be the reason of improved electrical conductivity.

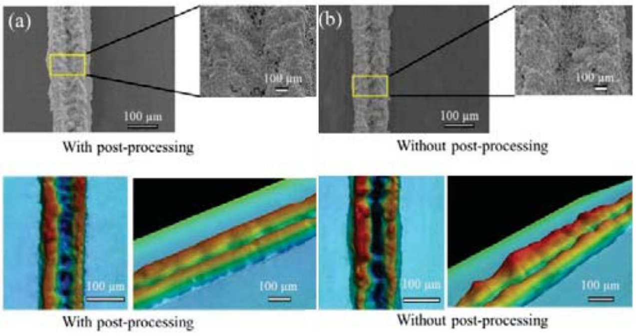

Fig. 8 SEM and 3D profiler images of fabricated Cu microline surface morphologies (a) with and (b) without post-processing.

3.3 Bubble dynamics

Figure 9 shows framewise capture microbubbles during LDSP. Evolution and growth of microbubbles during LDSP was found to be inevitable due to formation of byproduct gas as a result of photothermal reduction reaction during LDSP. Comprehensive investigation of bubble dynamics during LDSP can give insight to underlying mechanism of bubble formation and its significant effect on properties of fabricated conductive microstructures. LDSP experimental setup along with high speed camera coupled with zoom-in lens was used to capture framewise images of single microbubble. It should be noted that the laser was irradiated at a point on the substrate to capture growth of single microbubble. Figure shows growth of microbubble for a duration of ~1s at the rate of 1,219 frames per second. As can be seen, microbubble grows rapidly during its initial stage of bubble growth and stabilizes thereafter.

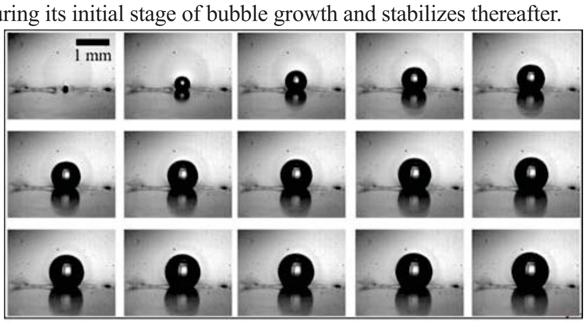

Fig. 9 A typical set of framewise captured images of microbubble growth during LDSP for a duration of ~1s at the rate of 1,219 frames per second.

4. Conclusions

An eco-friendly and particle-free Cu ionic solution to be used as precursor was prepared using DI water as solvent and ascorbic acid as reducing agent. Copper microlines were fabricated using 640 nm continuous wave laser with constant laser power and constant scanning speeds while the number of laser scans was varied. It was found that the resistance of the fabricated microlines decreases with increasing number of scans owing to increase in thickness of microline which becomes saturated after 20 LDSP scans. Apart from conductivity, mechanical durability of as prepared samples was also investigated through cyclic bending test. It was observed that resistance of Cu microlines increases with increase in bending cycles owing to formation of microcracks. To improve the mechanical durability, as prepared samples underwent laser post-processing. Cu microlines were reheated using same laser with different scanning parameters. It was found that change in resistance of the Cu microlines with post-processing after 1000 bending cycle was up to ~77% less than that without post-processing. Furthermore, post-processing also reduced the electrical resistance of the Cu microline by up to ~71%. SEM analysis and pull-off test revealed improvement in Cu-PET interfacial adhesion after post-processing which enhances the mechanical durability of the fabricated Cu microlines on PET. SEM analysis also revealed that the surface of copper microline became relatively smooth and average grain size increased by ~54% after post-processing which was the reason of reduces electrical resistance. In addition to fabrication and post-processing of Cu microstructure, growth of microbubbles was also captured using high speed camera in order to further investigate the underlying mechanism of bubble formation and its effect on properties of the conductive microstructures.

ACKNOWLEDGEMENT

Authors gratefully acknowledge the financial support from Ministry of Science and Technology (MOST) in Taiwan under grant Numbers: 109-2218-E-007-007, 109-2622-E-007-015-CC3, 110-2221-E-007-049, and 110-2218-E-007-053.

REFERENCES

1. J. Yeo *et al*., “Next generation non-vacuum, maskless, low temperature nanoparticle ink laser digital direct metal patterning for a large area flexible electronics,” PLoS One, vol. 7, no. 8, Aug. 2012.
2. M. T. Lee, D. Lee, A. Sherry, and C. P. Grigoropoulos, “Rapid selective metal patterning on polydimethylsiloxane (PDMS) fabricated by capillarity-assisted laser direct write,” J. Micromechanics Microengineering, vol. 21, no. 9, Sep. 2011.
3. Y. Sun, Y. Yin, B. T. Mayers, T. Herricks, and Y. Xia, “Uniform silver nanowires synthesis by reducing AgNO3 with ethylene glycol in the presence of seeds and poly(vinyl pyrrolidone),” Chem. Mater., vol. 14, no. 11, pp. 4736–4745, Nov. 2002.
4. S. L. Tsai, Y. K. Liu, H. Pan, C. H. Liu, and M. T. Lee, “The coupled photothermal reaction and transport in a laser additive metal nanolayer simultaneous synthesis and pattering for flexible electronics,” Nanomaterials, vol. 6, no. 1, Jan. 2016.
5. S. Siddharth, Y. Bin Chen, and M. T. Lee, “Eco-Friendly and Particle-Free Copper Ionic Aqueous Precursor for In Situ Low Temperature Photothermal Synthesizing and Patterning of Highly Conductive Copper Microstructures on Flexible Substrate,” Adv. Eng. Mater., vol. 24, no. 3, Mar. 2022.
6. S. Siddharth, S. L. Tsai, Y. Bin Chen, and M. T. Lee, “Opto-thermo-fluidic transport phenomena involving thermocapillary flow during laser microfabrication,” Int. J. Heat Mass Transf., vol. 162, Dec. 2020.

7. L. Lu, N. R. Tao, L. B. Wang, B. Z. Ding, and K. Lu, "Grain growth and strain release in nanocrystalline copper," J. Appl. Phys., vol. 89, no. 11 I, pp. 6408–6414, Jun. 2001.